MICROSTRUCTURE OF $Cu/ZnO/Al_2O_3$ METHANOL SYNTHESIS CATALYSTS STUDIED BY SCANNING AND TRANSMISSION ELECTRON MICROSCOPY AND DIFFRACTION METHODS

P. B. Himelfarb, G. W. Simmons, and K. Klier

Department of Metallurgy and Materials Engineering,
Department of Chemistry, and Center for Surface and
Coatings Research, Lehigh University,
Bethlehem, PA 18015

INTRODUCTION

Catalysts containing Cu/Zn/Al are well known active catalysts in methanol synthesis and the water-gas shift reaction, and have been described extensively in the literature (1-6). However, limited information is available on the elemental distributions in the various morphologies present in the many preparative variants of these catalysts. The understanding of these material properties and their relationship to synthesis activity is a primary goal in catalyst characterization. In the present work, transmission electron microscopy coupled with diffraction and elemental analysis was used to compare the chemical structure, morphology and elemental distribution in three different preparations of active Cu/Zn/Al catalysts.

EXPERIMENTAL

Two catalysts were prepared from Zn(II), Cu(II) and Al(III) acetate solution by coprecipitation with sodium carbonate at 90°C until a pH of 6.9 was reached to produce the compositions, Cu/Zn/Al equal to 54.4/24.3/23.3 and 27.3/63.6/9.0 at.% (prepared at Lehigh University). Another catalyst was similarly prepared from nitrate solution at 30°C to produce Cu/Zn/Al equal to 60.0/30.0/10.0 at.% (prepared at the University of Virginia). In all preparations, the precipitates were washed extensively, calcined in air at 350°C, and reduced at 250°C in a 60-70 cc/min 2% H_2/N_2 mixture for the time required for the stoichiometric reduction of CuO to Cu. Methanol synthesis activities were determined in a tubular fixed bed flow reactor equipped with pressure, temperature and flow rate controls (7,8). Methanol yields were determined by gas chromatography.

A Philips EM 400T transmission electron microscope (TEM) which included a scanning transmission mode (STEM) was used in the characterization studies. Samples were prepared by dispersing the catalyst powders in ethanol and placing a drop of the dispersion on a carbon coated titanium grid. Exposure time to air was minimized by preparing and transporting specimens in a N_2 filled glove bag. Energy dispersive X-ray analysis (EDS) for elemental identification and quantification was obtained in the manner described in references (4) and (9).

RESULTS

Methanol yields and respective surface areas for the catalysts studied are given in Table I. Data published for catalysts of similar

TABLE I

ACTIVITIES OF Cu/Zn/Al CATALYSTS

#	Catalyst Cu/Zn/Al at.%	Surface Area m^2/g	MeOH Yield g/g cat/hr
1	60.0/30.0/10.0[a]	54.2	1.35
2	52.4/24.3/23.3[b]	26.0	1.37
3	27.3/63.6/9.0[c]	61.8	1.55
4	67.0/33.0/0.0 (7)	7.4	0.41
5	30.0/70.0/0.0 (7)	39.3	1.35

[a]Prepared from nitrate solution, tested at 80 atm, 255°C, GHSV = 5600 hr^{-1}, $H_2/CO/CO_2$ = 69/27/4 (8).

[b]Prepared from acetate solution, tested at 75 atm, 250°C, GHSV = 5000 hr^{-1}, $H_2/CO/CO_2$ = 70/24/6 (10).

[c]Prepared from acetate solution, tested at 75 atm, 250°C, GHSV = 3750 hr^{-1}, $H_2/CO/CO_2$ = 70/24/6.

Cu/Zn compositions prepared without Al are given for comparison (7). As shown, high yields are maintained within a large variation in elemental composition. Elemental distribution, morphology, and chemical structure were determined for catalysts 1 and 3 (cf. Table I), and the results were compared with previously published data on catalyst 2 (10).

Two distinctly different morphologies were observed in both catalysts 1 and 3. One morphology was a platelet structure containing all three metals (Cu/Zn/Al) which gave a ZnO (0001) electron diffraction pattern, and appeared similar to the platelet morphology reported in catalyst 2 (10). The other morphology was lacelike and contained two metals (Cu/Zn) in the form of Cu and ZnO as determined by selected area diffraction (SAD). The lace-like morphology appeared similar to that found in an active Cu/ZnO (30/70 at.%) methanol catalyst (4,11). Micrographs of the ternary platelet and binary lace-like morphologies with corresponding dark field images from ZnO are given in Figures 1 and 2, respectively. The dark field micrographs show that the ZnO is more highly dispersed in the ternary platelet morphology. An SAD pattern of a platelet is given in Figure 3 which shows that the ZnO (0001) and Cu($\bar{1}$11) planes are parallel to the surface of the platelet. The epitaxial relationship between the Cu and ZnO shows that the Cu[0$\bar{2}$2] axis is parallel to the ZnO[1$\bar{2}$10] axis, which was similarly found in catalyst 2 (10) and in the Cu/ZnO (30/70 at.%) catalyst (4). Although the spot patterns appear to have been produced by single crystals, they originate from highly dispersed Cu and ZnO crystallites in crystallographic registry.

Crystal sizes of ZnO determined from TEM dark field images in the ternary platelet and binary lace-like morphologies, and Cu and ZnO crystallite sizes determined by X-ray diffraction line broadening are given in Table II for catalysts 1 and 3. Published data for catalyst 2 is also given for comparison (10). The microstructural similarities

TABLE II

MORPHOLOGIES AND CRYSTALLITE SIZES OF Cu/Zn/Al CATALYSTS

Catalyst #	Bulk Composition Cu/Zn/Al at.%	Abundance[a] of Platelets	ZnO by TEM (nm)[b]		XRD (nm)[c]	
			Platelet	Binary	ZnO	Cu
1	60.0/30.0/10.0	≅ 10%	2.6	9.1	7.0	12.4
2	52.4/24.3/23.3	≅100%	2-4	d	--	--
3	27.3/63.6/9.0	≅ 20%	2.6	11.9	12.3	8.9

[a]Given as the percent abundance of the ternary platelet morphology compared to the binary lace-like morphology.

[b]ZnO crystal sizes are an average of 100 measurements from TEM dark field measurements produced from the ZnO{10$\bar{1}$0}, {0002}, and {10$\bar{1}$1} reflections for the binary morphology, and from the ZnO(1$\bar{1}$00) diffraction spot for the platelet morphology.

[c]Crystallite sizes determined by X-ray diffraction line broadening using the Scherrer equation corrected for instrumental broadening (12); the Cu{111} and an average from the ZnO{10$\bar{1}$0}, {0002}, and {10$\bar{1}$1} reflections were used.

[d]Lace-like binary phase not present.

are striking in the platelet morphology in that the ZnO crystal sizes are essentially identical in catalysts 1, 2 and 3, and the epitaxial relation between Cu and ZnO was commonly observed. The higher average ZnO crystal sizes, determined by X-ray diffraction, reflect the higher concentration of the binary lace-like morphology which has larger ZnO crystallite sizes than the platelet morphology. In contrast to catalysts 1 and 3, catalyst 2 had large (greater than 0.1 μm) Cu particles and the binary lace-like morphology was not detected (10).

Elemental distributions in the platelets determined by EDS were: Catalyst 1 had the composition 4.5 ± 3.8 at.% Cu, 75.5 ± 2.8 at.% Zn, and 20.0 ± 1.9 at.% Al from 27 measurements, and catalyst 3 platelets contained 24.5 ± 7.9 at.% Cu, 56.6 ± 5.8 at.% Zn, and 18.9 ± 7.8 at.% Al from 23 measurements. No Al was detected in the binary lace-like morphology in catalyst 3, and in catalyst 1 a weak Al peak was sometimes observed which corresponded to less than 1 wt.% in the binary morphology. No evidence of crystalline Al-containing compounds was found by either X-ray or electron diffraction analysis. EDS analysis of platelets in catalyst 2 resulted in 8 ± 2 at.% Cu, 50 ± 5 at.% Zn, and 42 ± 4 at.% Al (10).

DISCUSSION

Comparison of the methanol yields for the three Al-containing catalysts studied shows that active catalysts can be prepared from either acetate or nitrate solutions, and that high concentrations of

Cu are not necessary for high activity.

The activity of catalyst 2 has been attributed to the platelet morphology because the only other morphology present was large inactive Cu particles, as reported earlier (10). Since methanol yields for catalysts 1, 2 and 3 are similar, and the relative abundance of the platelet and lace-like morphologies varied significantly (see Table II), the activity of the platelet and lace-like morphologies must be comparable. Binary Cu/ZnO catalysts have been prepared with high methanol synthesis activity (see catalyst 5 in Table I). The activity of the binary lace-like morphology in catalysts 1 and 3, which contains little or no Al, supports the view that an Al_2O_3 component serves basically as a structural promoter (2).

A comparison of catalysts 2 and 3 (which have similar activities but dramatically different Cu/Zn ratios) to catalysts of similar Cu/Zn ratios prepared without Al (see catalysts 4 and 5 in Table I) shows that the addition of Al widens the Cu/Zn compositional range which can be used to produce an active catalyst. This is a result of the increased dispersion of Cu and ZnO occurring in the Al-containing catalysts.

In summary, active Cu/Zn/Al methanol synthesis catalysts do not require high concentrations of copper. Three basic morphologies — large Cu particles (greater than 0.1 μm), Cu/Zn/Al polycrystalline platelets, and a binary Cu/ZnO morphology can be produced in different amounts by variations in the initial elemental concentrations and preparation conditions. The ternary platelet and binary lace-like morphologies are active in methanol synthesis, which is believed to be a result of the intimate dispersion of the Cu and ZnO crystallites in both morphologies. The Al component, which appears amorphous, is a structural support in the platelets, and widens the Cu/Zn ratio range for which high dispersion of Cu and ZnO can be obtained.

ACKNOWLEDGMENTS

This research was supported by the U.S. Department of Energy through the Pittsburgh Energy Technology Center (Grant No. DE-FG22-80PC30265).

REFERENCES

(1) Kung, H. H., Catal. Rev. - Sci. Eng. 22(2), 235 (1980).

(2) Klier, K., Adv. Cat. 31, 243 (1982).

(3) Shimomura, K., Ogawa, K., Oba, M, Kotera, Y., J. Catal. 52, 191 (1978).

(4) Mehta, S., Simmons, G. W., Klier, K., Herman, R. G., J. Catal. 57, 339 (1979).

(5) Natta, G., (Emmett, P. H., ed.) "Catalysis Volume III," Reinhold Publishing Corp., New York, 1955, p.349.

(6) Imperial Chemical Industries, "Catalyst Handbook," Springer-Verlag, New York, Billing and Sons Ltd., 1970.

(7) Herman, R. G., Klier, K., Simmons, G. W., Finn, B. P., Bulko, S. B., J. Catal. 56, 407 (1979).

(8) Bieser Jr., A. L., Ph.D. Thesis, University of Virginia, Charlottesville, VA (1983).

(9) Himelfarb, P. B., Master's Thesis, University of Virginia, Charlottesville, VA (1983).

(10) Herman, R. G., Simmons, G. W., Klier, K., Proceedings of the 7th International Congress on Catalysis, Tokyo, June 30 - July 4, 1980 (1981).

(11) Cullity, B. D., "Elements of X-Ray Diffraction," 2nd edition, Addison-Wesley Publishing Co., Inc. 1978, p.284.

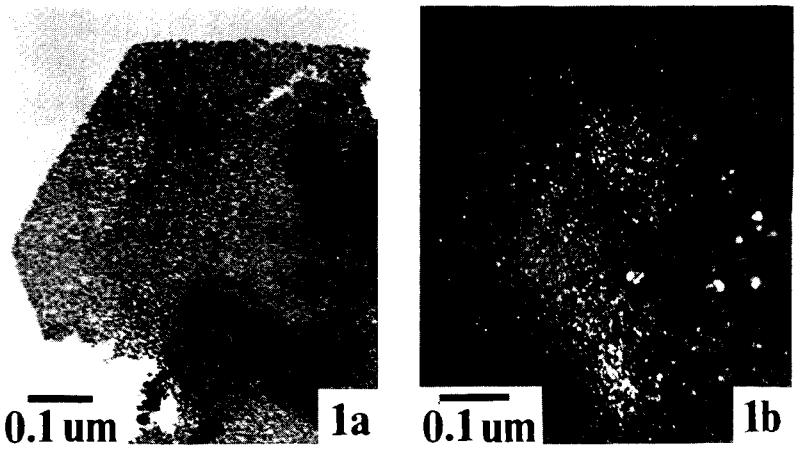

Figure 1. Electron micrographs of ternary platelet morphology in catalyst 3 (Cu/Zn/Al at.% = 27.3/63.6/9.0). (a) Bright field image, (b) dark field image from a ZnO($1\bar{1}00$) diffraction spot (see Fig. 3).

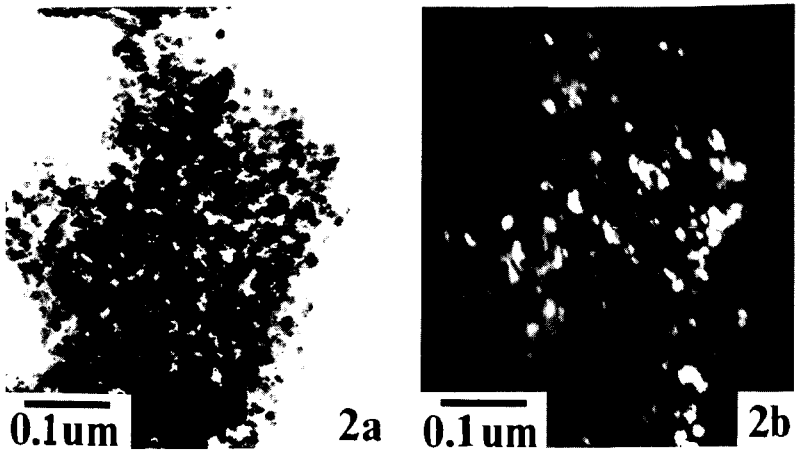

Figure 2. Electron micrograph of binary lace-like morphology in catalyst 3 (Cu/Zn/Al at.% = 27.3/63.6/9.0). (a) Bright field image, (b) dark field image from ZnO{$10\bar{1}0$}, {0002}, and {$10\bar{1}1$} diffraction rings.

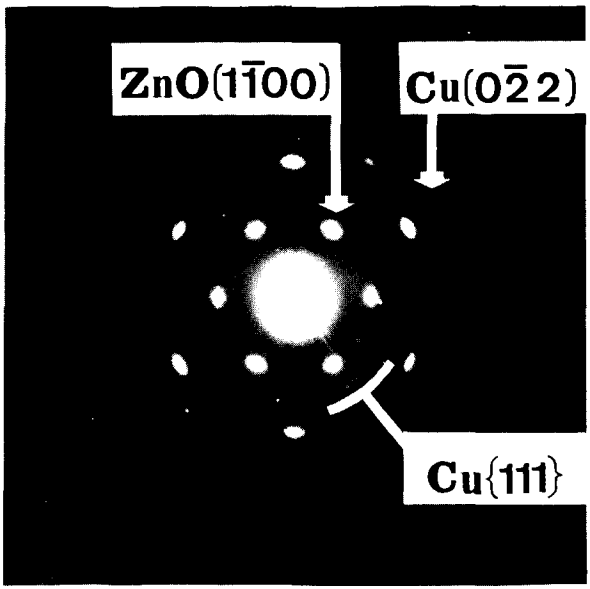

Figure 3. Selected area diffraction pattern of the ternary platelet morphology in catalyst 3 (Cu/Zn/Al at.% = 27.3/63.6/9.0) showing randomly oriented Cu, from the Cu{111} ring pattern, and single crystal patterns of Cu($\bar{1}$11) and ZnO(0001), defined by the Cu(0$\bar{2}$2) and ZnO(1$\bar{1}$00) diffraction spots.